2024 European Control Conference (ECC)
June 25-28, 2024. Stockholm, Sweden

# Physics-Informed Road Monitoring and Suspension Control Using Crowdsourced Vehicle Data

Yanbing Wang, Karl Berntorp, and Marcel Menner

*Abstract*— **This paper proposes a technology for road-shape monitoring using crowdsourced vehicle data. The technology uses vehicle measurements and a dynamics model in a statistical estimation framework with a kernel model approximating the road shape. The rationale for considering the vehicle dynamics for road monitoring is that the same road yields different measurements/oscillations for different vehicle types. Next, this paper shows how to use such estimated road shape and vehicle dynamics for semi-active suspension control with the objective to improve passenger comfort. Results using the high-fidelity simulator CarSim show that the proposed technology (i) only needs a few vehicles for estimating the road shape, (ii) can improve passenger comfort by semi-active suspension control, and (iii) is robust to model mismatch indicating the applicability to a real-world scenario.**

## I. Introduction

Road monitoring is required for maintenance, but it is a time consuming and expensive task. On the other hand, scores of vehicles traverse a city's road infrastructure daily. The scores of vehicles have onboard sensors such as inertial measurement units (IMUs). Such vehicles are capable of collecting data at no additional expense and can communicate with each other and the city's infrastructure wirelessly. While the data collected from each individual vehicle is expected to be noisy, crowdsourcing offers a viable alternative to expensive technology as noise is averaged out as a sufficient number of vehicles traverses the road.

In this paper, we propose a technology that uses crowdsourcing to estimate the road shape using multiple vehicles that traverse the road. In particular, our technology combines IMU vehicle measurements with a model of the vehicle dynamics to infer the road shape. The rationale for leveraging the vehicle's dynamics is that while the road shape remains constant for all vehicles, the measurements collected vary between different vehicles as function of their velocity and the type of vehicle. The proposed technology uses a kernel function to parametrize the road shape and a vehicle dynamics model that relates the road shape to IMU measurements of the vehicle. Further, the proposed technology formulates the road estimation as statistical estimation problem, in which the parameters of the kernel function representing the road shape are updated episodically after a vehicle traversed the road segment. Specifically, we formualte the statistical estimation problem using a recursive episodical Kalman filter-based implementation. Next, we leverage the estimated road shape in combination with a vehicle's dynamics for semi-active suspension control with the objective of improving passenger comfort. Simulation results show that the road shape can be estimated with only a few vehicles traversing the road segment. Further, results using the high-fidelity simulator CarSim show that the proposed algorithm can deal with the gap between the control-oriented vehicle dynamics model and a high-fidelity vehicle model, i.e., sim-to-sim gap. These results indicate the applicability of the proposed technology to a real-world vehicle.

Mitsubishi Electric Research Laboratories (MERL), 201 Broadway, Cambridge, MA, 02139, USA (e-mail: karl.o.berntorp@ieee.org).

### A. Related Works

Road-monitoring is a well-studied problem using different types of approaches. The works [1]–[8] employ smartphones and their accelerometers to monitor the road conditions, and a review of some of the approaches using smartphones is detailed in [9]. The papers [10]–[14] focus on anomaly detection while [15], [16] take a crowdsourced approach. Most previous work formulate the road-monitoring problem as a classification problem with no vehicle dynamics model. While [17] uses a dynamic model, it is based on a truck-trailer model with different focus from our paper. Different from most previous work on road-surface monitoring, we focus on relatively more obvious surface anomalies such as bumps and potholes, which impact the ride quality, and we furthermore show how our method can be applied to semi-active suspension control. In this paper, we fuse past driving history with present data to accurately and quickly predict road conditions and anomalies based on a flexible kernel representation.

### B. Problem Formulation

In this paper, we address the following two problems.

*Problem 1: Road Monitoring:* We frame the road-monitoring problem as an episodical estimation task, where the road shape impacts the vehicle behavior. This is achieved by leveraging vehicle dynamics in combination with vehicle measurements to infer the road shape. Further, we leverage crowdsourced data to estimate the road shape more efficiently by considering the different dynamics of multiple vehicles traversing the same road.

*Problem 2: Suspension Control:* After the road-profile estimation, we leverage the road shape for semi-active suspension control to improve the comfort of passengers while driving through the road segment. In this context, semi-active suspension control selects the best suspension parameters from a set of possible suspension settings with respect to some comfort criterion.

## II. Preliminaries

### A. Half-Car Model

Let the half-car dynamics model be written as

$$\dot{x}(t) = Ax(t) + Fd(t) + F_n(t), \tag{1}$$

with $x = [z_c, \phi, z_f, z_r, \dot{z_c}, \dot{\phi}, \dot{z_f}, \dot{z_r}]^T$, $d = [g_f, g_r, \dot{g_f}, \dot{g_r}]^T$, and

$$A = \left[\begin{array}{c|c} 0 & I \\ \hline K_s & C_s \end{array}\right] \in \mathbb{R}^{8\times 8}, F = \left[\begin{array}{c|c} 0 & 0 \\ \hline K_t & C_t \end{array}\right] \in \mathbb{R}^{8\times 4}, \tag{2}$$

where $z_c$ is the vertical chassis displacement, $\phi$ is the pitch angle, and $z_f$ and $z_r$ are the front and rear suspension displacement, respectively; $g_f$ and $g_r$ define the road elevation at the front and real wheel, respectively; $F_n(t)$ defines the gravity vector; $K_s \in \mathbb{R}^{4\times 4}$ is the suspension stiffness matrix, $C_s \in \mathbb{R}^{4\times 4}$ is the suspension damping matrix, $K_t \in \mathbb{R}^{4\times 2}$ is the tire stiffness matrix, and $C_t \in \mathbb{R}^{4\times 2}$ is the tire damping matrix. Further, we discretize the dynamics using the sampling period $\delta t$:

$$x_{k+1} = A_d x_k + F_d d_k + F_{n,k}, \tag{3}$$

with $A_d = I + \Delta t A$, $F_d = \Delta t F$, and $F_{n,k} = \Delta t F_n(t)$.

### B. Kernel Model and Regression

We use a kernel model for learning the road shape as a flexible function approximator. A kernel relates two data points, $x, x' \in \mathbb{R}$ by $k(x, x') : \mathbb{R} \times \mathbb{R} \to \mathbb{R}$. Throughout, we use a common choice of kernel, the radial basis function:

$$k(x, x') = \exp\left(-\gamma(x - x')^2\right), \tag{4}$$

where $\gamma$ corresponds to the lengthscale. Note that $k(x, x') = 1$ if $x = x'$ and $k(x, x') \to 0$ for $x$ far away from $x'$. Next, let

$$k(x, X) = \begin{bmatrix} k(x, x_1) & k(x, x_2) & \dots & k(x, x_M) \end{bmatrix} \in \mathbb{R}^{1\times M},$$
$$X = \begin{bmatrix} x_1 & x_2 & \dots & x_M \end{bmatrix} \in \mathbb{R}^{n_d \times M},$$

and

$$K_{xx} = \begin{bmatrix} k(x_1, x_1) & k(x_1, x_2) & \dots & k(x_1, x_M) \\ k(x_2, x_1) & k(x_2, x_2) & \dots & k(x_2, x_M) \\ \vdots & \vdots & \ddots & \vdots \\ k(x_M, x_1) & k(x_M, x_2) & \dots & k(x_M, x_M) \end{bmatrix}.$$

Given $M$ training data points with input $x \in \mathbb{R}^{n_d \times M}$ and the corresponding training output $Y \in \mathbb{R}^M$, we can define a predictor $f(x) : \mathbb{R}^{n_d} \to \mathbb{R}$ by

$$f(x) = k(x, x)\left(K_{xx} + \sigma_0^2 I\right)^{-1} Y. \tag{5}$$

## III. Road Monitoring

We model the road shape using a kernel function in Sec. II-B. In this paper, we study a 2D vehicle and road, i.e., we use the half-car model in Sec. II-A and model the longitudinal road shape. However, expanding the proposed technology to a 3D vehicle model and include the lateral road is straightforward. Hence, the shape representing the road elevation at a longitudinal position $\delta(p)$ is given by

$$\delta(p) = k(p, x)\left(K_{xx} + \sigma_0^2 I\right)^{-1} Y, \tag{6}$$

where $x = [x_1, ..., x_M]$ and $Y = [y_1, ..., y_M]^T$ relate to longitudinal positions along the road segment and their associated elevation. Note that $x$ is given in this context and does not change during the road estimation. Hence, we formulate the road-monitoring problem as a recursive estimation of $Y$. As we formulate the problem in an episodical manner, $Y$ is adapted after each vehicle has traversed the road segment.

*Remark 1:* Here $\delta(p)$ provides a mapping from the position on the road to the corresponding displacement values, e.g., potholes and bumps.

*Remark 2:* The multiple vehicles traversing the road segment need not travel at the same velocity. In fact, the accelerations experienced by the passengers vary greatly as a function of the vehicle's velocity. Such variations, however, are explicitly accounted for by considering the vehicle dynamics.

As the kernel model is differentiable,

$$\dot{\delta}(p) = \frac{\partial \delta(p)}{\partial t} = \frac{\partial \delta(p)}{\partial p}\frac{\partial p}{\partial t} = \frac{\partial \delta(p)}{\partial p} v(t) \tag{7a}$$

where $\frac{\partial p}{\partial t} = v(t)$ and

$$\frac{\partial k(x, x')}{\partial x} = \frac{\partial \exp\left(-\gamma(x - x')^2\right)}{\partial x} \tag{7b}$$
$$= \exp\left(-\gamma(x - x')^2\right)\frac{\partial\left(-\gamma(x - x')^2\right)}{\partial x} \tag{7c}$$
$$= -2\gamma(x - x')\exp(-\gamma(x - x')^2) \tag{7d}$$
$$=: g(x, x') \tag{7e}$$

Hence, the road grade $\dot{\delta}$ at position $p(t)$ is given by

$$\dot{\delta}(p(t)) = v(t) g(p(t), x)\left(K_{xx} + \sigma_0^2 I\right)^{-1} Y. \tag{8}$$

The advantage of using this formulation is that (i) the road shape and its derivative are parametric functions that are linear in the unknown parameters $Y$ and (ii) the kernel model is very flexible in its approximation capabilities.

### A. Combining Kernel Road with Half-Car Vehicle Model

Using the kernel model of the road shape, we can express the dynamical system (3) with

$$d_k = \begin{bmatrix} \delta(p_k + l_f) \\ \delta(p_k - l_r) \\ \dot{\delta}(p_k + l_f) \\ \dot{\delta}(p_k - l_r) \end{bmatrix} \tag{9a}$$
$$= \begin{bmatrix} k(p_k + l_f, x) \\ k(p_k - l_f, x) \\ v_k g(p_k + l_f, x) \\ v_k g(p_k - l_r, x) \end{bmatrix}\left(K_{xx} + \sigma_0^2 I\right)^{-1} Y \tag{9b}$$
$$:= G(p_k) Y. \tag{9c}$$

Finally, let $z_k$ be the vehicle measurements as a subset of $x_k$ with $z_k = C x_k$.

Overall, using the half-car model in (3) and the kernel model in (9),

$$x_{k+1} = A_d x_k + F_d G(p_k) Y + w_k \tag{10a}$$
$$z_k = C x_k + v_k, \tag{10b}$$

where $w_k \sim \mathcal{N}(0, Q)$ and $v_k \sim \mathcal{N}(0, R)$ are zero-mean Gaussian-distributed process and measurement noise, respectively.

### B. Episodical Formulation for Road Monitoring

As we formulate the estimation problem as a recursive episodical task, we use (9) as the basis to develop a stacked representation, i.e.,

$$X_\tau = \begin{bmatrix} x_0 \\ \vdots \\ x_{N-1} \end{bmatrix}_\tau = \bar{A}_\tau x_{0,\tau} + \bar{B}_\tau Y_\tau + \bar{A}^w_\tau W_\tau \tag{11a}$$
$$Z_\tau = \begin{bmatrix} z_0 \\ \vdots \\ z_{N-1} \end{bmatrix}_\tau = \bar{C}_\tau X_\tau + V_\tau \tag{11b}$$
$$= \bar{C}_\tau \bar{B}_\tau Y_\tau + \bar{C}_\tau \bar{A}_\tau x_{0,\tau} + \bar{C}_\tau \bar{A}^w_\tau W_\tau + V_\tau \tag{11c}$$
$$:= H_\tau Y_\tau + \nu_\tau, \tag{11d}$$

where $\tau$ denotes the episode, i.e., each $\tau$ represents a vehicle traversing the road segment. Here, $W_\tau \sim \mathcal{N}(0, Q_W)$, $V_\tau \sim \mathcal{N}(0, Q_V)$, $\bar{A}_\tau$, $\bar{B}_\tau$, $\bar{A}^w_\tau$, $\bar{C}_\tau$, $H_\tau = \bar{C}_\tau \bar{B}_\tau$ , and $\nu_\tau = \bar{C}_\tau \bar{A}_\tau x_{0,\tau} + \bar{C}_\tau \bar{A}^w_\tau W_\tau + V_\tau$, are chosen according to (11a). Such a stacked formulation is standard in the predictive control literature.

### C. Kalman Filter-based Implementation

We formulate the episodical road-estimation problem as

$$Y_{\tau+1} = \lambda \cdot Y_\tau + \omega_\tau \tag{12a}$$
$$Z_\tau = H_\tau Y_\tau + \nu_\tau, \tag{12b}$$

with $\omega_\tau \sim \mathcal{N}(0, Q_\omega)$ and $\nu_\tau \sim \mathcal{N}(\mu_\nu, R_\nu)$ from (11d), i.e., $\mu_\nu = \bar{C}_\tau \bar{A}_\tau x_{0,\tau}$ and $R_\mu = (\bar{C}_\tau \bar{A}^w_\tau) Q_W (\bar{C}_\tau \bar{A}^w_\tau)^T + Q_V$, where (12a) defines a prior in the road shape estimation and (12b) drives the adaptation of the road shape by means of the measurements taken, i.e., $Z_\tau$, and by means of the vehicle dynamics, i.e., embedded in $H_\tau$. In (12a), $\lambda \in (0, 1]$ defines a forgetting factor.

Algorithm 1 summarizes the road-monitoring procedure. In this formulation, we estimate the kernel model parameters $Y$ that parametrize the differentiable road-shape model $\delta(p)$ from multiple vehicles' vertical dynamics measurements using a Kalman filter. This Kalman filter-based estimation is implemented with episodic updates, i.e., $Y$ is updated with the batch measurements of each car after traveling the road segment, instead of at each time step.

*Remark 3 (Theoretical Properties):* Note that observability of the proposed Kalman filter-based implementation depends on the available vehicle measurements as well as on the type of vehicle. In particular, we can show that a diverse set of vehicle increases the rank of the observability matrix.

**Algorithm 1:** Kalman Filter for Episodic Update

**Initialize:** $\hat{Y}_{0|0}, P_{0|0}$
**for** *each* $\tau$ **do**
**Predict**
$\hat{Y}_{\tau|\tau-1} = \lambda \hat{Y}_{\tau-1|\tau-1}$
$P_{\tau|\tau-1} = \lambda^2 P_{\tau-1|\tau-1} + Q_\omega$

**Update**
$K_\tau = P_{\tau|\tau-1} H_\tau^T (H_\tau P_{\tau|\tau-1} H_\tau^T + R_\nu)^{-1}$
$\hat{Y}_{\tau|\tau} = \hat{Y}_{\tau|\tau-1} + K_\tau (Z_\tau - H_\tau \hat{Y}_{\tau|\tau-1})$
$P_{\tau|\tau} = (I - K_\tau H_\tau) P_{\tau|\tau-1}$

Moreover, even if the estimation problem is not observable, it is easy to see that any $\lambda \in (0, 1)$ makes the road-shape estimation problem detectable. Hence, $Y$ remains bounded and does not drift.

## IV. Semi-Active Suspension Control

Next, we show how to use an estimated road for semi-active suspension control. The approach is again based on leveraging the dynamics of the vehicle. The idea is to vary the suspension calibration, i.e., springs and dampers, to stabilize the vertical oscillation due to the combined influence of the road and vehicle dynamics.

Mathematically, we formulate the calibration as an optimization problem to select the best suspension setting, e.g., in terms of riding comfort, from a range of choices according to our estimation of the road profile $Y$ from Sec. III. The suspension setting is characterized by the stiffness and damping parameters $\theta = [k_{fs}, k_{rs}, c_{fs}, c_{rs}]^T$, where for each vehicle, we select the best one amongst a finite set of possible settings $\Theta$. The trial index $\tau$ is dropped in the control formulations for simplicity.

We use a comfort measure $l(X)$, which can include vertical accelerations, pitch rate, pitch angle, or a combination thereof. Note that the comfort measure $l(X)$ can also include an uncertainty quantification, which can be used to optimize w.r.t. worst-case performance or similar robustness measures. To emphasize dependencies on suspension parameters, we rewrite $\bar{A}, \bar{B}$ as $\bar{A}_\theta$ and $\bar{B}_\theta$. Hence, the optimization problem is given by

$$\min_{\theta, X} \quad l(X) \tag{13a}$$
$$\text{s.t.} \quad X = \bar{A}_\theta x_0 + \bar{B}_\theta Y \tag{13b}$$
$$\theta \in \Theta. \tag{13c}$$

In practice, (13) can easily be solved by evaluating the comfort measure $l(X)$ for all possible $\theta \in \Theta$ and choosing $\theta^\star$ that minimizes $l(X)$.

## V. Simulation Results

In this section we provide road-shape estimation results (Sec. V-A) and using Carsim we subsequently assess its impact on control performance (Sec. V-B).

TABLE I: Vehicle parameters for the different vehicle types used to generate the road-shape estimation results.

| | Description | Sedan | Pickup | Hatchback | SUV |
|---|---|---|---|---|---|
| $m_c$ | Chassis mass (kg) | 1100 | 1137.2 | 400 | 1225 |
| $m_f$ | Front wheel mass (kg) | 46 | 28 | 28 | 31 |
| $m_r$ | Rear wheel mass (kg) | 46 | 28 | 28 | 31 |
| $I_{yy}$ | Chassis pitch inertia (kg·m$^2$) | 2500 | 2957 | 375 | 1700 |
| $k_{fs}$ | Front susp. stiffness (N/m) | 8000 | 198000 | 18000 | 7000 |
| $k_{rs}$ | Rear susp. stiffness (N/m) | 8400 | 198000 | 18000 | 7000 |
| $k_{ft}$ | Front tire stiffness (N/m) | 10000 | 2000 | 6000 | 6000 |
| $k_{rt}$ | Rear tire stiffness (N/m) | 10000 | 2000 | 6000 | 6000 |
| $c_{fs}$ | Front susp. damping (N·s/m) | 1000 | 1000 | 1000.8 | 1000.8 |
| $c_{rs}$ | Rear susp. damping (N·s/m) | 1000 | 1000 | 1000.8 | 1000.8 |
| $c_{ft}$ | Front tire damping (N·s/m) | 100 | 600 | 300 | 300 |
| $c_{rt}$ | Rear tire damping (N·s/m) | 100 | 600 | 300 | 300 |
| $l_f$ | CoM to front susp. (m) | 1.4 | 1.4 | 1.1 | 1.33 |
| $l_r$ | CoM to rear susp. (m) | 1.2 | 2.55 | 1.25 | 1.81 |

### A. *Road Shape Estimation*

We investigate the impact of vehicle types, speeds, and measurement configuration on the estimation accuracy. In the simulation setup, the crowdsourced vehicle data originate from four different vehicle types: sedans, SUVs, pickup trucks, and hatchbacks. Each type corresponds to a different set of suspension, tire-stiffness, and damping coefficients. Table I shows the different sets of parameters.

To estimate the continuous road function $\delta(p)$ according to the kernel model described in Sec. I-B, we need the hyperparameter $\gamma$ in the kernel function (4) and the spatial discretization that characterizes the modeling resolution for the road function (6). Here, we set $\gamma = 4$ and the spatial resolution to be 10 uniform sampling points per meter on a 100-meter road segment, i.e., $x = [0.1, ..., 100] \in \mathbb{R}^{1\times 1000}$. Hence, the road parameters $Y \in \mathbb{R}^{1000}$ and the kernel matrix $K_{xx} \in \mathbb{R}^{1000\times 1000}$. These values are selected to balance the resolution needed for understanding of the road surface and computational time, and are design choices that in our experience do not significantly impact the estimation results.

The parameter vector $Y$ is estimated using Algorithm 1. Figs. 1 and 2 display qualitative results of a "bumpy" road and a sinusoidal road, respectively, where we use the chassis vertical acceleration ($\ddot{z}_c$) and the pitch rate ($\dot{\phi}$) of up to 50 vehicles of random types to estimate the two different road profiles. The black line represents the ground-truth road elevation as a function of the traveled distance, while the orange line represents the estimated road profile using to 1, 5, 20, and 50 vehicles, respectively. The shaded region represents $\pm 1$ estimated standard deviation. Clearly, as the number of vehicles increase, the estimation becomes more and more accurate and for 50 vehicles (subplot d) the road profile can be accurately estimated. Note, however, that for many applications, e.g., suspension control and road-condition monitoring, the rate of change of the road profile is of more interest. From Figs. 1 and 2, for the considered scenario 5 vehicles is sufficient to detect the road bumps.

Overall, the estimation results improve with an increasing number of vehicles, even when the initial assumption of the road is random. However, when the road is mostly flat and

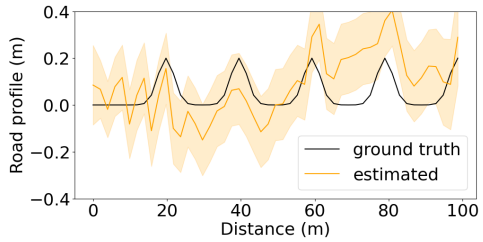


(a) 1 iteration

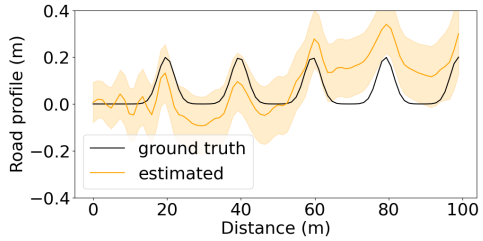


(b) 5 iterations

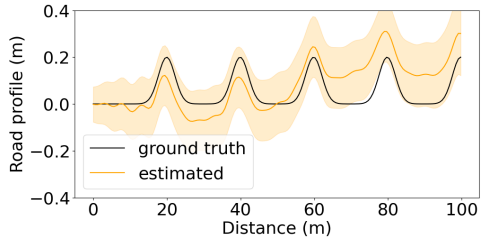


(c) 20 iterations

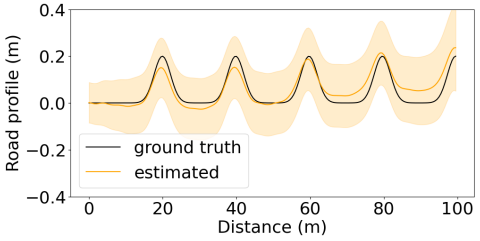


(d) 50 iterations

Fig. 1: Estimated road profile using up to 50 vehicles randomly drawn from a mixed fleet of sedans, SUVs, pickup trucks, and hatchbacks. Each vehicle travels at a random speed between 10-40m/s. Although the slope is drifting, the road bumps can be identified.

occasionally has road bumps (Fig. 1), the KF is unable to correct the drift in slope, because constant road slopes do not excite the suspension dynamics, and cannot be measured by chassis acceleration and pitch rate alone without additional position measurements (e.g., using a chassis vertical displacement sensor). Nonetheless, the bumps that contribute to the suspension response can still be accurately identified. A continuously varying road shape (e.g., the sinusoidal road in Fig. 2) excites the system due to a nonzero derivative of the road shape and the estimation therefore is more accurate.

### B. *Application to Active Suspension Control*

We present the proposed road-profile estimation to assess its relevance for suspension control. We have a set of different suspension parameters. We use the half-car vehicle model (see Sec. II-A) to estimate the road shape and subsequently

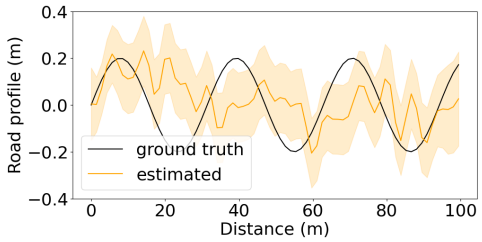


(a) 1 iteration

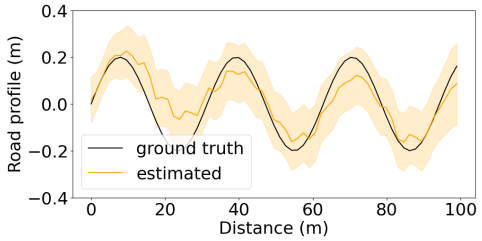


(b) 5 iterations

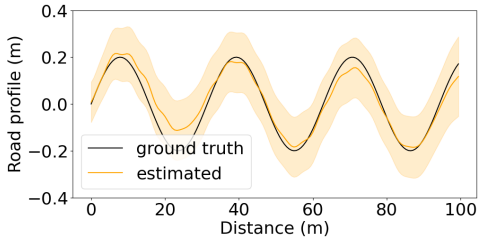


(c) 20 iterations

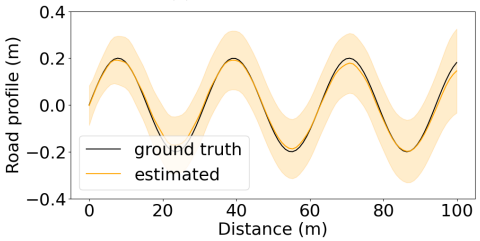


(d) 50 iterations

Fig. 2: Estimated road profile using up to 50 vehicles randomly drawn from a mixed fleet of sedans, SUVs, pickup trucks and hatchbacks. Each vehicle travels at a random speed between 10-40m/s. The sine-wave road can be accurately identified.

the vehicle state. Based on the estimates, we solve (13) to find the best possible parameter vector $\theta^\star \in \Theta$.

We use the high-fidelity vehicle dynamics simulator CarSim [18] to validate our approach. The chassis, tire, and environment models used in CarSim are of substantially higher fidelity than the half-car model employed in the proposed control scheme. Hence, being able to execute the applied algorithms using a simplified control-oriented model against the high-fidelity simulator indicates the robustness of the method and suggests the applicability to a physical vehicle. For reproducibility, we provide the selected modules and simulation parameters in the Appendix. In the generated results, the control loop is executing at 10Hz.

Fig. 3 shows a sequence of snapshots from Carsim of the suspension behavior without (left column) and with (right column) semi-active suspension control. Starting from a flat

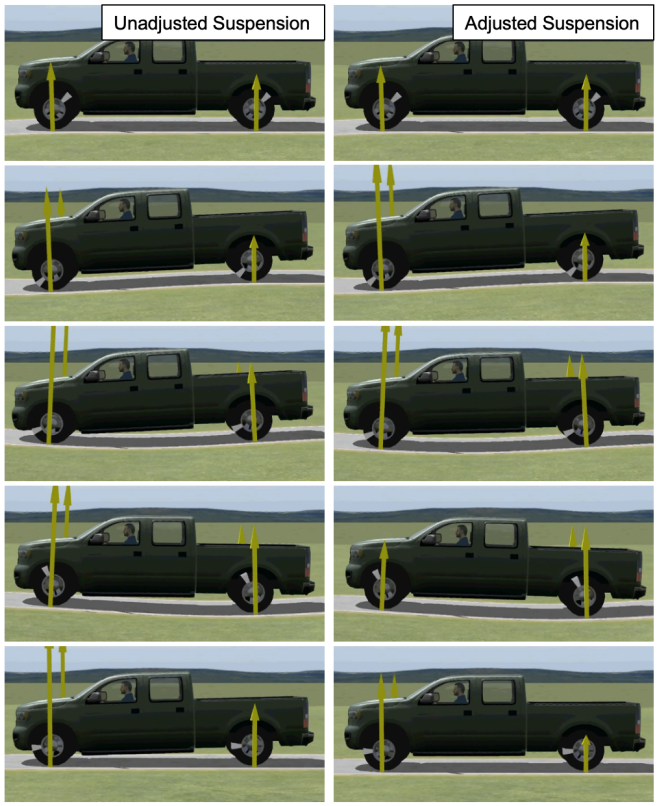


Fig. 3: Carsim results without (left column) and with (right column) active suspension control by solving (13) based on the estimated road shape and vehicle states. Active suspension leads to a smoother ride (see the maximum normal forces).

road (first row), the vehicle enters a bump (second to fourth rows) and finally exits the bump (fifth row). The size of the normal forces on the wheels are reflected by the magnitude of the arrows for respective wheel. Clearly, judging by the normal forces the travel comfort is improved for the maneuver, and the maximum normal forces exerted on the wheels are decreased as a result of the suspension parameter adaptation.

Fig. 4 shows the corresponding vertical velocities and pitch rates. The maximum values of the vertical velocity and pitch rate, and the corresponding rate of changes, decrease with the adjusted suspension, indicating a smoother ride.

## VI. Conclusions

This paper proposed a framework for road monitoring and semi-active suspension control. The proposed framework combined vehicle measurements and vehicle dynamics in order to efficiently estimate the shape of the road. The rationale for leveraging vehicle dynamics is that the road shape remains constant for all vehicles, however, the accelerations experiences reflected in the measurements depend on the type of vehicle and its suspension. The road-estimation problem was framed as a statistical estimation problem using a recursive implementation. Further, the semi-active suspension controller uses the vehicle dynamics as well as the estimated road shape in order to select the suspension calibration

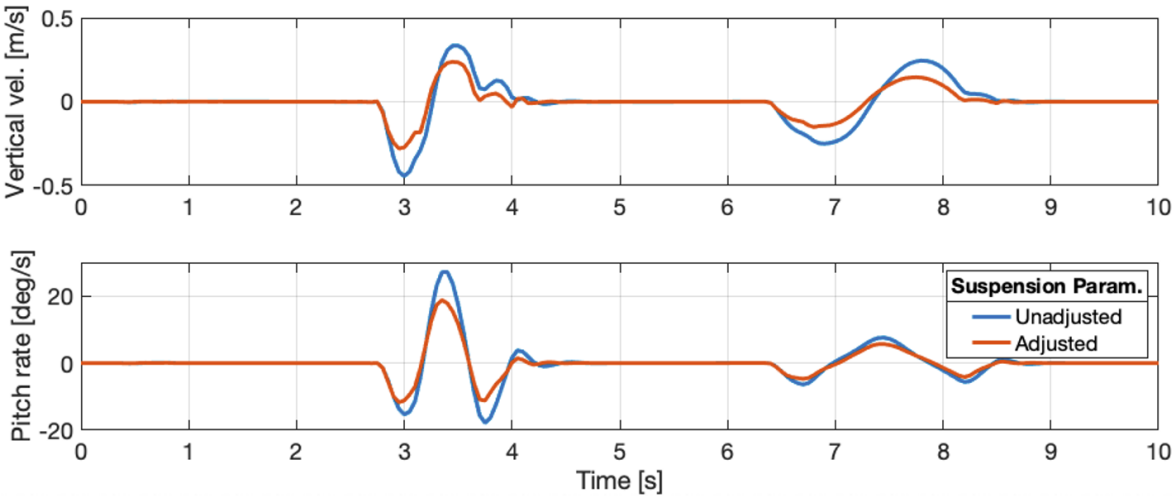


Fig. 4: Vertical velocities and pitch rates corresponding to the scenario in Fig. 3.

that optimizes a comfort criterion. Simulation results show that the road shape can be estimated using less than 50 vehicles. Further, results using the high-fidelity simulator CarSim indicate that the proposed framework is robust to the differences between the control-oriented vehicle model and a real vehicle. In particular, after only 10 simulated vehicles in CarSim, the semi-active suspension controller reduces accelerations/oscillation of the vehicle due to road bumps by more than 35%.

## Appendix: Half-Car Model

Here, we describe the half-car model in detail, i.e.,

$$K_s = \begin{bmatrix} \frac{-(k_{fs}+k_{rs})}{m_c} & \frac{l_r k_{rs} - l_f k_{fs}}{m_c} & \frac{k_{fs}}{m_c} & \frac{k_{rs}}{m_c} \\ \frac{l_r k_{rs} - l_f k_{fs}}{I_{yy}} & \frac{-\left(l_f^2 k_{fs} + l_r^2 k_{rs}\right)}{I_{yy}} & \frac{-l_f k_{fs}}{I_{yy}} & \frac{-l_r k_{rs}}{I_{yy}} \\ \frac{k_{fs}}{m_f} & \frac{l_f k_{fs}}{m_f} & \frac{-(k_{fs}+k_{ft})}{m_f} & 0 \\ \frac{k_{rs}}{m_r} & \frac{-l_r k_{rs}}{m_r} & 0 & \frac{-(k_{rs}+k_{rt})}{m_r} \end{bmatrix},$$

$$C_s = \begin{bmatrix} \frac{-(c_{fs}+c_{rs})}{m_c} & \frac{l_r c_{rs} - l_f c_{fs}}{m_c} & \frac{c_{fs}}{m_c} & \frac{c_{rs}}{m_c} \\ \frac{l_r c_{rs} - l_f c_{fs}}{I_{yy}} & \frac{-\left(l_f^2 c_{fs} + l_r^2 c_{rs}\right)}{I_{yy}} & \frac{-l_f c_{fs}}{I_{yy}} & \frac{-l_r c_{rs}}{I_{yy}} \\ \frac{c_{fs}}{m_f} & \frac{l_f c_{fs}}{m_f} & \frac{-(c_{fs}+c_{ft})}{m_f} & 0 \\ \frac{c_{rs}}{m_r} & \frac{-l_r c_{rs}}{m_r} & 0 & \frac{-(c_{rs}+c_{rt})}{m_r} \end{bmatrix},$$

and

$$K_t = \begin{bmatrix} 0 & 0 \\ 0 & 0 \\ \frac{k_{ft}}{m_f} & 0 \\ 0 & \frac{k_{rt}}{m_r} \end{bmatrix}, C_t = \begin{bmatrix} 0 & 0 \\ 0 & 0 \\ \frac{c_{ft}}{m_f} & 0 \\ 0 & \frac{c_{rt}}{m_r} \end{bmatrix}.$$

## References


[1] J. Eriksson, L. Girod, B. Hull, R. Newton, S. Madden, and H. Balakrishnan, "The pothole patrol: using a mobile sensor network for road surface monitoring," in *Proceedings of the 6th international conference on Mobile systems, applications, and services*, pp. 29–39, 2008.

[2] P. Mohan, V. N. Padmanabhan, and R. Ramjee, "Nericell: rich monitoring of road and traffic conditions using mobile smartphones," in *Proceedings of the 6th ACM conference on Embedded network sensor systems*, pp. 323–336, 2008.

[3] K. Chen, M. Lu, X. Fan, M. Wei, and J. Wu, "Road condition monitoring using on-board three-axis accelerometer and GPS sensor," in *Int. ICST conference on communications and networking in China*, pp. 1032–1037, 2011.

[4] M. Perttunen, O. Mazhelis, F. Cong, M. Kauppila, T. Leppänen, J. Kantola, J. Collin, S. Pirttikangas, J. Haverinen, T. Ristaniemi, *et al.*, "Distributed road surface condition monitoring using mobile phones," in *Int. Conf. ubiquitous intelligence and computing*, pp. 64–78, 2011.

[5] A. Vittorio, V. Rosolino, I. Teresa, C. M. Vittoria, P. G. Vincenzo, and D. M. Francesco, "Automated sensing system for monitoring of road surface quality by mobile devices," *Procedia - Social and Behavioral Sciences*, vol. 111, pp. 242–251, 2014.

[6] H. Sharma, S. Naik, A. Jain, R. K. Raman, R. K. Reddy, and R. B. Shet, "S-road assist: Road surface conditions and driving behavior analysis using smartphones," in *2015 International Conference on Connected Vehicles and Expo (ICCVE)*, pp. 291–296, 2015.

[7] A. S. El-Wakeel, J. Li, M. T. Rahman, A. Noureldin, and H. S. Hassanein, "Monitoring road surface anomalies towards dynamic road mapping for future smart cities," in *2017 IEEE global conference on signal and information processing (GlobalSIP)*, pp. 828–832, 2017.

[8] T. Lee, C. Chun, and S.-K. Ryu, "Detection of road-surface anomalies using a smartphone camera and accelerometer," *Sensors*, vol. 21, no. 2, p. 561, 2021.

[9] S. Sattar, S. Li, and M. Chapman, "Road surface monitoring using smartphone sensors: A review," *Sensors*, vol. 18, no. 11, p. 3845, 2018.

[10] Y.-c. Tai, C.-w. Chan, and J. Y.-j. Hsu, "Automatic road anomaly detection using smart mobile device," in *conference on technologies and applications of artificial intelligence*, 2010.

[11] D. Luo, J. Lu, and G. Guo, "Road anomaly detection through deep learning approaches," *IEEE Access*, vol. 8, pp. 117390–117404, 2020.

[12] X. Zhang, Z. Yang, C. Wu, W. Sun, Y. Liu, and K. Xing, "Robust trajectory estimation for crowdsourcing-based mobile applications," *IEEE Transactions on Parallel and Distributed Systems*, vol. 25, no. 7, pp. 1876–1885, 2013.

[13] N. Silva, V. Shah, J. Soares, and H. Rodrigues, "Road anomalies detection system evaluation," *Sensors*, vol. 18, no. 7, p. 1984, 2018.

[14] Y.-A. Daraghmi, T.-H. Wu, and T.-U. İk, "Crowdsourcing-based road surface evaluation and indexing," *IEEE Transactions on Intelligent Transportation Systems*, vol. 23, no. 5, pp. 4164–4175, 2022.

[15] N. Sabir, A. A. Memon, and F. K. Shaikh, "Threshold based efficient road monitoring system using crowdsourcing approach," *Wireless Personal Communications*, vol. 106, no. 4, pp. 2407–2425, 2019.

[16] F. Abbondati, S. A. Biancardo, R. Veropalumbo, and G. Dell'Acqua, "Surface monitoring of road pavements using mobile crowdsensing technology," *Measurement*, vol. 171, p. 108763, 2021.

[17] J. Keenahan, E. J. OBrien, P. J. McGetrick, and A. Gonzalez, "The use of a dynamic truck–trailer drive-by system to monitor bridge damping," *Structural Health Monitoring*, vol. 13, no. 2, pp. 143–157, 2014.

[18] Mechanical Simulation, "CarSim," *https://www.carsim.com*, ver. 2021.0.